Acta Pharmacologica Sinica

www.nature.com/aps

ARTICLE

GDF11 promotes wound healing in diabetic mice via stimulating HIF-1α-VEGF/SDF-1α-mediated endothelial progenitor cell mobilization and neovascularization

Ying Zhang[1], Yi-yuan Zhang[1], Zhen-wei Pan[1], Qing-qi Li[1], Li-hua Sun[1], Xin Li[2], Man-yu Gong[1], Xue-wen Yang[1], Yan-ying Wang[1], Hao-dong Li[1], Li-na Xuan[1], Ying-chun Shao[1], Meng-meng Li[1], Ming-yu Zhang[1], Qi Yu[1], Zhange Li[1], Xiao-fang Zhang[1], Dong-hua Liu[1], Yan-meng Zhu[1], Zhong-yue Tan[1], Yuan-yuan Zhang[1], Yun-qi Liu[1], Yong Zhang[1], Lei Jiao[1] and Bao-feng Yang[1,3]

Non-healing diabetic wounds (DW) are a serious clinical problem that remained poorly understood. We recently found that topical application of growth differentiation factor 11 (GDF11) accelerated skin wound healing in both Type 1 DM (T1DM) and genetically engineered Type 2 diabetic *db/db* (T2DM) mice. In the present study, we elucidated the cellular and molecular mechanisms underlying the action of GDF11 on healing of small skin wound. Single round-shape full-thickness wound of 5-mm diameter with muscle and bone exposed was made on mouse dorsum using a sterile punch biopsy 7 days following the onset of DM. Recombinant human GDF11 (rGDF11, 50 ng/mL, 10 μL) was topically applied onto the wound area twice a day until epidermal closure (maximum 14 days). Digital images of wound were obtained once a day from D0 to D14 post-wounding. We showed that topical application of GDF11 accelerated the healing of full-thickness skin wounds in both type 1 and type 2 diabetic mice, even after GDF8 (a muscle growth factor) had been silenced. At the cellular level, GDF11 significantly facilitated neovascularization to enhance regeneration of skin tissues by stimulating mobilization, migration and homing of endothelial progenitor cells (EPCs) to the wounded area. At the molecular level, GDF11 greatly increased HIF-1α expression to enhance the activities of VEGF and SDF-1α, thereby neovascularization. We found that endogenous GDF11 level was robustly decreased in skin tissue of diabetic wounds. The specific antibody against GDF11 or silence of GDF11 by siRNA in healthy mice mimicked the non-healing property of diabetic wound. Thus, we demonstrate that GDF11 promotes diabetic wound healing via stimulating endothelial progenitor cells mobilization and neovascularization mediated by HIF-1α-VEGF/SDF-1α pathway. Our results support the potential of GDF11 as a therapeutic agent for non-healing DW.

Keywords: diabetic wound; GDF11; endothelial progenitor cell; neovascularization; HIF-1α; VEGF/SDF-1α

Acta Pharmacologica Sinica (2023) 44:999–1013; https://doi.org/10.1038/s41401-022-01013-2

INTRODUCTION

Diabetes mellitus (DM) is a disease accompanied by multiple complications such as cardiomyopathy, diabetic nephropathy, vasculopathy and endothelial dysfunction. The impaired wound healing such as foot ulcer is a serious complication of DM, which could ultimately lead to amputation, and another serious complication that tremendously increases the social and medical burdens is non-healing chronic cutaneous wound. The skin, as the largest organ of the human body accounting for ~15% of total body weight in adult humans, is the utmost frontline protective barrier serving its primary responsibility to the immune system against varying environmental hazards [1]. When the structural integrity of the skin is compromised, its primary function as the body defense mechanism is impaired, which can result in serious morbidity and mortality [1–3]. Yet skin damage is a frequently encountered problem and a wide variety of insults can result in cutaneous wounds, of which non-healing, chronic wound is typically developed from complications of DM [3]. It is estimated that currently one-third of the adult population or more than 200 million people worldwide suffer from DM, which may well climb up to >360 million people by 2030 [4, 5]. Diabetic wound (DW) developing into diabetic foot ulcers (DFU) is the leading cause of hospital admission in diabetic patients, which can eventually lead to limb loss contributing to a 3-year mortality rate of 76% [6]. Developing therapeutic approaches that accelerate healing of DW have therefore become a prioritized task of both fundamentalists and clinicians. Whilst a number of technologies have been exploited for the treatment of DW over the past decades [7], cost-effective therapy for such conditions has been lacking.

[1]Department of Pharmacology (State-Province Key Laboratories of Biomedicine-Pharmaceutics of China, Key Laboratory of Cardiovascular Medicine Research, Ministry of Education), College of Pharmacy, Harbin Medical University, Harbin 150081, China; [2]Department of Cardiovascular Sciences, School of Engineering, University of Leicester, Leicester, UK and [3]Department of Pharmacology and Therapeutics, Melbourne School of Biomedical Sciences, Faculty of Medicine, Dentistry and Health Sciences, University of Melbourne, Melbourne, VIC, Australia
Correspondence: Lei Jiao (jiaolei116@163.com) or Bao-feng Yang (yangbf@ems.hrbmu.edu.cn)
These authors contributed equally: Ying Zhang, Yi-yuan Zhang

Received: 14 June 2022 Accepted: 12 October 2022
Published online: 8 November 2022

Among the various therapeutic approaches, polypeptide growth factors (GFs), a class of biological mediators that promote cell growth, proliferation, and differentiation by binding to their respective specific cell surface receptors, have recently been scrutinized for their efficacy in improving wound healing [8, 9]. Many in vitro studies suggest that GFs are released by platelets (e.g. PDGF and EGF) or by activated macrophages (e.g. PDGF and bFGF), the cells that are required for normal wound repair [10, 11]. GFs can also stimulate neovascularization, extracellular matrix production and degradation and cytokine release [12, 13]. For example, platelet-derived growth factor (PDGF) plays a significant role in blood vessel formation, the growth of blood vessels from already-existing blood vessel tissue. Effects of PDGF to accelerate tissue repair under conditions of impaired wound healing have been demonstrated in animal models [14] and human patients [15]. To date, recombinant PDGF (also known as becaplermin) is the only recombinant cytokine growth factor approved by the U.S. Food and Drug Administration to promote wound closure via topical application [15].

Recently, growth differentiation factor 11 (GDF11; also known as bone morphogenetic protein 11/BMP11) has gripped great attention from scientific communities worldwide owing to the still-ongoing debate on whether it really is an elixir of youth. In the years of 2013 and 2014, three high-profile studies identified GDF11 as a blood circulating anti-aging factor based on the results showing its higher abundance in young than in old mice in parabiosis procedures [16–18]. These studies provided evidence that GDF11 depletion is associated with aging processes, and GDF11 replacement can reverse age-related cardiac hypertrophy and dysfunction in mouse skeletal muscle, and to improve the cerebral vasculature and mitigate the neurodegenerative process of the aging mouse brain. These findings were soon disputed in 2015 by a study demonstrating the contrary: GDF11 increases with age and has deleterious effects on skeletal muscle regeneration and can exacerbate rather than rejuvenate skeletal muscle injury in old animals, being a pro-aging factor [19]. Further in 2016, another study claimed that GDF11 does not rescue aging-related pathological hypertrophy [20]. Yet, in the same year, these contrary results were evidenced to be the result of a flawed assay that was detecting immunoglobulin but not GDF11, and the original conclusion that GDF11 reverses age-related cardiac hypertrophy holds true [21]. A more recent study expanded the beneficial role of GDF11 in the heart from cardiac hypertrophy to ischemia-reperfusion injury by enhancing myocardial regeneration [22]. In the most recent study, GDF11 was reported to improve neovascularization-related growth parameters in endothelial progenitor cells isolated from peripheral blood [23], which is in good agreement with the earlier study showing the ability of GDF11 to promote the cerebral vascularization [16]. These studies, together with other published results, prompted us to propose that GDF11 might play a role in the healing process of DW via accelerating neovascularization, a key step in the wound healing process [24–26]. Recently, our research group reported that both truncated and natural GDF11s could accelerate skin wound healing in both Type 1 DM (T1DM) and genetically engineered Type 2 diabetic *db/db* (T2DM) mice partly via stimulating dermal fibrosis [27]. It is known that the process of DW healing involves multiple mechanisms and the aim of the present study was to investigate the underlying physiological, cellular and molecular mechanisms of GDF11 on healing of small full-thickness skin wound. Our results generated strong evidence in support of the potential of GDF11 as a therapeutic agent for non-healing DW.

MATERIALS AND METHODS

Study approval

The experimental protocols involving the use of animals in this study were approved by the Animal Care and Use Committee of Harbin Medical University (HMUIRB20170035), and are conformed to the Guidelines for the Care and Use of Laboratory Animals set forth by the US National Institutes of Health (NIH Publication No. 85–23, revised 1996).

Mouse model of type 1 diabetes mellitus (T1DM)

Kunming male mice (1012 weeks of age) weighing 29–31 g were obtained from Beijing Vital River Laboratory Animal Technology Co., Ltd (Beijing, China). The mice were kept in an animal house with controlled temperature of 23 ± 1 °C and humidity of 55% ± 5% on 12 h dark–light artificial cycle under standard conditions with food and water available *ad libitum* for 1 week before the experiment procedures.

Mice were given a single intraperitoneal injection of 180 μg/g streptozotocin (STZ; Sigma, St Louis, MO, USA) dissolved in 0.1 M sodium citrate buffer (pH 4.5), and immediately after the injection they were supplied with glucose water for 12 h. Fasting blood glucose (FBG) levels were measured seven days after streptozotocin injection using Roche Glucometer (Roche, Mannheim, Germany) and T1DM model was considered successfully established with FBG levels >11.5 mM (Supplementary Fig. S1a). The Control group was treated with an equal volume of 0.1 M sodium citrate buffer. The animals were randomly divided into two groups for subsequent experimental measurements, including T1DM and T1DM + rGDF11.

Mouse model of type 2 diabetes mellitus (T2DM)

Male BKS wild-type ($n = 6$) and male T2DM mice ($n = 12$) homozygous for leptin-receptor-deficient *db/db* ($Lepr^{db/db}$) aged 7~8 weeks were purchased from Nanjing BioMedical Research Institute of Nanjing University (NBRI; China). T2DM was verified with random FBG levels >30 mM (Supplementary Fig. S1b).

Mouse model of wound

Wound was developed in mice seven days following the onset of DM. Mice were narcotized by avertin (2%, 10 μL/g; Sigma, St. Louis, MO, USA) and their dorsal hair was cleared up. Once an adequate anesthesia had been achieved, a single round-shape full-thickness wound of 5-mm diameter with muscle and bone exposed was created on mouse dorsum using a sterile punch biopsy. Following these procedures, animals were single-cage bred. Sacrificial animals were excluded from the wound analysis and following experiments.

Topical application of GDF11

Recombinant human GDF11 (rGDF11) was purchased from PeproTech (Rocky Hill, NJ, USA). The agent was dissolved in 0.1% (*w/v*) bovine serum albumin (BSA) buffer and stored at −80 °C until use. Mice were randomly divided into three groups: Normal+BSA (Ctl-BSA as a vehicle control group), DM + BSA (as the DM control group) and DM + rGDF11 (DM-rGDF11 as the test group). rGDF11 (50 ng/mL, 10 μL) or BSA (0.1%, *w/v*) was topically applied onto the wound area for the DM-GDF11 group. Drug application was carried out twice a day until epidermal closure (maximum 14 days). Digital images of wound were obtained once a day from day 0 to day 14 post-wounding for monitoring the time course of wound healing. The area surrounded by visible edge of dermis was defined as the wound area. Wound size was determined using Image-ProPlus (IPP Version 5.0.2.9; Media Cybernetics, Rockville, MD, USA). The wound tissues were harvested for further analyses on days 1, 5, 10 and 14 post-wounding. Randomization and blinding were adopted and dead mice were excluded.

The antibody of GDF11, PX-478 and AAV-sgGDF11 virus topical application on wound

Anti-GDF11 antibody (Cat#sc-81952, Santa Cruz, CA, USA) for topical application against the function of endogenous GDF11 was

purchased from Santa Cruz (Santa Cruz, CA, USA), which can react with human, rat, and mice. AAV8 viral vector that contains the shRNA for silencing GDF11 expression (AAV8-sgGDF11) was provided by LandM Biological Technology Co, Ltd (Guangzhou, China). The anti-GDF11 antibody (10 μg/wound) or AAV8-sgGDF11 virus (1×10^6 genome containing particles (GC)/wound) was hypodermically injected into the wound area three days prior to (day 0) and six days after creation of wound (day 6). HIF-1α inhibitor PX-478 was purchased from MedChem Express (Cat#HY-10231, Shanghai, China, 20 μM, 100 μL/wound), and hypodermically injected into the wound area one day prior to (day 0) creation of wound.

Wound-healing analysis

A single lens reflex camera (Nikon D300; Nikon, Melville, NY) with standardized exposure and focal length was used to record the wound area once a day (9:00 am) from the first day when the wound was opened (assigned as Day 0), the vertical distance from the lens to the wound was kept as 30 cm. The size of the remaining unhealed-wound area was measured based on the image using the Image Analyzing Tool IPP.

Photographs were analyzed to calculate percentages of wound closure using the image analysis software IPP. Wound-healing curve was constructed with the rate of wound healing expressed as the percentage of unhealed-wound area. The Residual Wound Area = Rn/R1, where R1 and Rn denote the remaining area on postoperative day 1 and n (n = from day 2 to the day with complete wound healing), respectively.

Percentage of wound closure at each time point was calculated as: WC = [(WAd0 – WAICdn)/WAd0] × 100, where WC stands for % wound closure, WAd0 for wound area on Day 0, WAdn for wound area on Day n with n = from Day 2 to the Day 14. Half wound-closure time (WCT50) was determined by curve fitting to the data points in the wound-closure curve using the equation: $WC = WAd0 + (WAd14 - WAd0)/(1 + 10^{WCT50-dn}) \times k$ (slope).

Histopathological analysis

Mice were euthanatized with an intraperitoneal injection of avertin (0.3 mL; Sigma) on days 5 and 14. Following the euthanasia, the entire wound and a rim of surrounding unwounded skin margins (~10 mm) were excised to the depth of the retro-peritoneum. Samples were washed and fixed in 4% paraformaldehyde for at least 24 h, followed by dehydration in serial concentrations of ethanol (80%, 90%, 95% and 100%) for 2 h. The samples were then sectioned through the center of the lesion to obtain the largest possible diameter of the wound and underwent routine paraffin processing. The preparations were serially sectioned at a thickness of 5 μm and the sections were placed in an incubator at 60 °C for 30 min to remove paraffin wax. The tissue sections were stained with hematoxylin and eosin (H&E) for viewing histopathological changes or with CD31 (Abcam, Cambs, UK) for viewing vessels. The widest sections obtained were measured and then photographed using a mounted digital camera (Olympus DP72; Olympus, Melville, NY, USA).

Chick chorioallantoic membrane neovascularization assay

Fertilized E6 chicken embryos (48 ± 5 g) were cleaned with 0.1% benzalkonium bromide and preincubated with 85% humidity at 37.5 °C for 2 days. After disinfection of the shell center outside the air sac with 0.1% benzalkonium bromide, a hole highlighted with marker pen was buffed and drilled gently over the air sac with a nipper to avoid breaking the shell. The vascular zone was identified on the chorioallantoic membrane (CAM). Saline, 0.1% BSA, or rGDF11 (50 ng/mL) was added. Upon sealing of the openings with a sterile flexible packing film, the eggs were incubated with 85% humidity at 37.5 °C for three days. Finally, a mixture of methanol and acetone (1:1 in volume) was directly added to immerse and fix the blood vessels. The CAM was cut and spread on glass slide, and the blood vessels were viewed and photographed. The total vessel number was quantified by ImageJ software. Relative number of vessels (%) = vessel number per membrane area in cm^2 − vessel number (Ctl) per membrane area in cm^2/vessel number (Ctl) × membrane area in cm^2 × 100%.

Immunofluorescence analysis

Frozen sections were placed on glass slides, dried at 50 °C for 1 h, and then rinsed in PBS. CD34 was detected with an anti-mice CD34-specific antibody (Abcam, Cambs, UK) at a 1:200 dilution. The secondary antibody was an Alexa-Fluor 488-linked anti-mouse IgG antibody (Molecular Probes, Eugene, OR, USA) used at a 1:500 dilution. Murine kinase insert domain receptor or VEGF receptor 2 (KDR) was detected with a rabbit monoclonal antibody (Abcam, UK) at a 1:200 dilution. Alexa-Fluor 594-linked anti-rabbit IgG antibody (Molecular Probes) was used as the secondary antibody at a 1:500 dilution. All blocking steps were performed with SuperBlock reagent (Biogenex, San Ramon, CA, USA). Processed sections were mounted in mounting media (VectaShield; Vector Laboratories, Burlingame, CA, USA) and viewed on an Olympus BX51 epifluorescent microscope. For quantification of CD34-KDR co-positive cells, pictures were analyzed under ×600 magnification, and total positive cells per high-power field (HPF) were counted by an examiner in a blinded manner.

RNA extraction

Total RNA was extracted from skin tissues surrounding the wounds using Trizol reagent according to the manufacturer's instructions (Invitrogen, Camarillo, CA, USA) followed by phenol/chloroform extraction. The integrity of extracted RNA was quantified by denaturing gel showing discrete 28 s and 5 s bands without smear, and the concentrations were measured by NanoDrop ND-8000 (Thermo Fisher Scientific, Waltham, MA, USA) to ensure the RNA/DNA ratio of 1.8–2.0.

Quantitative real-time polymerase chain reaction (qRT-PCR)

The first strand Complementary DNA was synthesized using SuperScript III Reverse Transcriptase (Transgene, Beijing, China), according to manufacturer's protocol. Real-time PCR was performed using SYBR Green PCR Master Mix (Transgene) to quantify the target genes on the ABI7500 fast Real-Time PCR system (Applied Biosystems). β-actin was used as an internal control in each sample. The transcript levels of vascular endothelial growth factor (VEGF), stromal cell-derived factor-1 alpha (SDF-1α), hypoxia-inducible factor-1 alpha (HIF-1α), GDF11, GDF8, col1a1, col3a1 and β-actin were detected using the primers listed in Supplementary Table 1. The specificity of the amplified product was monitored by its melting curve. Relative standard curves were generated by plotting the threshold value (Ct) versus the log of the total amount of cDNA that was added to the reaction. All reactions were performed in triplicate. The level of gene expression was calculated using the $2^{-\Delta\Delta Ct}$ method, where $\Delta Ct = Ct_{\text{target gene}} - Ct_{\text{endogenous}}$ and $\Delta\Delta Ct = \Delta Ct_{\text{individual sample}} - \Delta Ct_{\text{reference sample}}$.

Western blot analysis

Total protein was extracted from tissues surrounding the wounds at various time points (days 5 and 10) by lysis buffer (Beyotime, Beijing, China) supplemented with 0.5 mM PMSF and 2 mM sodium orthovanadate. Protein concentration was assayed using the BCA analysis kit (Beyotime, Beijing, China). Equal amounts of protein (100 μg) were subjected to SDS-PAGE electrophoresis and then transferred onto PVDF membranes (Pall Life Science, Pensacola, FL, USA). After blocking with 5% milk, the membranes were probed with specific antibodies against GDF11 (Cat#-MAB19581, R&D Systems, Minnesota, USA), VEGF (Cat#ab46154, Abcam, Cambs, UK), HIF-1α (Cat#3716, Cell signaling, Danvers, MA, USA), SDF-1α (Cat#GTX45117, GeneTex, TX, USA), p-Smad2/3 (Cat#8828s, CST, Boston, USA), Smad2/3 (Cat#8685s, CST, Boston,

USA), TGF-β (Cat#3711, CST, Boston, USA), and β-actin (ZSGB-Bio, Beijing, China), respectively. Western blotting was run under moderate reducing conditions, and for the detection of monomeric GDF11 protein (12.5 kDa), the protein samples were pretreated with SDS-PAGE loading buffer containing 2-hydroxy-1-ethanethiol (P1041, Solarbio, Beijing, China) to create more stringent reducing conditions. Images of Western blot bands were obtained using the Oddessy Infrared Imaging System (LI-COR Biosciences, Lincoln, NE, USA) and the band density was quantified using Odyssey 3.0 software (LI-COR Bioscience) for each group and normalized to β-actin bands. The values from the test groups were normalized to those from the control groups.

Culture and treatment of bone marrow derived endothelial progenitor cells (EPCs)

Mice were euthanatized, and bone marrow was isolated from their femurs and tibias. The bone marrow samples were then subjected to density gradient centrifugation to isolate mononuclear cells. The mononuclear cells were plated into fibronectin-coated flasks and plates. EPCs were cultured with EGM-2 MV bullet kit medium (Lonza, Basel, Switzerland) supplemented with 5% fetal bovine serum, recombinant human rhEGF, rhFGF-B, rhVEGF, rhIGF-1, ascorbic acid, and heparin. The cells that were double positive for DiI-labeled acetylated LDL (DiI-acLDL; Thermo Fisher Science, Walthem, MA, USA) and ULEX Europadus Agglutinin-1 (FITC-UEA-1; Sigma) by direct fluorescent staining were identified as EPCs as reported before (Supplementary Fig. S9) [28]. The cultured cells isolated from control mice were incubated with rGDF11 (Peprotech, Rocky Hill, NJ, USA, 50 ng/mL). In another set of experiments, EPCs were incubated with BSA (0.1% *w/v*).

To silence GDF11 expression in EPCs, specific siRNA against mouse GDF11 or Silencer Select Negative Control (Invitrogen, Shanghai, China) was transfected into EPCs using X-treme (Roche, Mannheim, Germany), as per manufacturer's instructions.

Flow cytometry analysis of EPC numbers

Mice were anesthetized on the fifth day after creation of a dermal wound on the dorsal skin. Blood samples were collected from inferior vena cava. Lymphocytes and mononuclear cells were isolated using peripheral lymphocyte isolation kit (Cat#P8620; Solarbio, Beijing, China). The wound skin tissue was digested by type II collagenase. The solution with mixed cells was then incubated with Alexa-Fluor 488-linked anti-CD34, Phycoerythrin-linked anti-KDR, and APC-linked anti-CD133 antibody mix (Becton, Dickinson and Company, Franklin Lake, NJ, USA) at 4 °C in the dark for 30 min. Follow cytometry was employed to quantify the CD34/KDR/CD133 positive cells (or EPCs).

Trans-endothelial migration by transwell assay

EPCs migration was detected using transwell assay. EPCs were cultured in the upper chamber of a 24-transwell insert (8.0 μm pores; Corning, NY, USA). Before each experiment, the cells were treated with 50 ng/mL rGDF11, BSA, or transfected with siGDF11 or other constructs. Then EPCs were harvested and resuspended in EBM-2 medium. EPCs suspension was added to the upper chamber of the transwell and 0.5 mL EGM-2 medium to the lower chamber. Cells were cultured at 37 °C for 24 h. The EPCs traversing from the upper to the lower chamber of the transwell were recorded by photographs taken by Olympus E330, and were counted by Image-ProPlus.

Neovascularization assay in vitro

The in vitro angiogenic capability of EPCs was determined by Matrigel tube formation assay. Briefly, 24-well plates were coated with growth factor-reduced Matrigel (Corning, New York, USA, 100 μL/per well). EPCs pretreated with GDF11 (50 ng/mL), BSA (50 ng/mL), GDF11 siRNA, or NC were plated in 200 μL EGM-2 medium or medium containing GDF11 at a cell density of 5×10^4 cells/well, and incubated with 5% CO_2 at 37 °C for 12 h for tube formation. Images of tubes in each well were taken using an inverted microscopy (Olympus E330, Olympus). Lengths of the tubes were calculated by Image J and the tube areas by Image-ProPlus.

Micro-PET/CT of dermal lesion

Fourteen days after wound, the mice were administered developer Exitron nano 12000CT contr. Agent (Miltenyi Biotec, Bergisch Gladbach, Germany) via tail vein injection. The animals were anesthetized 150 min after injection. The skin of the wounded area was dissected. The specimens were scanned by PET/CT (SuperArgus 2 R PET/CT; Sedecal, Madrid, Spain) in the Micro-CT Core Laboratory in the Experimental Center of the Fourth Affiliated Hospital of Harbin Medical University. The CT settings were: FOV 120 × 350 mm, X-ray tube voltage 50 kV and current 300 μA, 768 × 486 pixels detectors, 30-ms exposure time, 4 × 4 binning, and 50 μm spatial resolution.

Culture and treatment of human umbilical vein endothelial cells (HUVEC)

Human umbilical vein endothelial cells (HUVECs) were cultured in DMEM high glucose medium (BioInd, Kibbutz Beit Haemek, Israel) with 10% fetal bovine serum (FBS), 100 IU/mL penicillin, and 100 μg/mL streptomycin in humidified air with 5% CO_2 at 37 °C. HUVECs at passage 4–8 were used for transfection of siGDF11.

Effect of rGDF11 on capillary-like tube formation in HUVECs

The effect of rGDF11 on capillary-like tube formation was determined as previously described in detail [29]. Briefly, HUVECs were plated on the plate precoated with Matrigel (0.1 mL; Corning, NY). The cells were treated with rGDF11 (50 ng/ml) or BSA and incubated under 5% CO_2 and 95% humidified airflow at 37 °C for 24 h. The cells were washed with Dulbecco's phosphate-buffered saline (DPBS), followed by treatment with 2 μg/mL Calcein AM (Cat#ab141420; Abcam, Cambs, UK). After incubation for an additional 30 min, images of the cells were captured using a microscope at ×100 magnification. The total number of tubes was calculated by ImageJ software. Each data point was obtained in triplicate. Relative number of tubes = ((test tube number/cell number − Ctl tube number/cell number)/(Ctl tube number/cell number)) × 100%.

Statistics

Results are expressed as mean ± SEM. Statistical analysis was performed using statistical software SPSS (version 19.0; SPSS, Chicago, IL, USA). Comparisons among multiple groups were analyzed by one-way analysis of variance (ANOVA) followed by Dunnett's multiple comparison test. Comparisons between the groups were conducted using the Student's *t*-test. Values of $P < 0.05$ were considered statistically significant.

RESULTS

GDF11 accelerates diabetic wound healing (DWH) in both type 1 and 2 diabetic mice

To explore the role of GDF11 in diabetic would healing (DWH), we began with the development of a mouse model of type 1 DM (T1DM) induced by injection of streptozotocin (STZ), and only male mice were used in our study to minimize the possible confounding influence due to gender differences. Successful establishment of T1DM was verified by monitoring the changes of fasting blood glucose (FBG) levels. As shown in Supplementary Fig. S1a, FBG was drastically elevated from a baseline level of 4.62 ± 0.2 mM to 29.4 ± 0.5 mM 7 days after STZ injection in T1DM mice, whereas in the vehicle control counterparts, the baseline values remained unaltered within the same timeframe. We then confirmed the bioactivities of recombinant GDF11

(rGDF11) used in our experiments by showing the remarkable activation of Smad2/3 in human umbilical vein endothelial cells (HUVECs), as previously indicated by the increased levels of phosphorylated Smad2/3 proteins (p-Smad2/3) (Supplementary Fig. S2) [30].

We next created a wound on the dorsal skin of each mouse using a biopsy punch. Consistent with our previous findings [27], GDF11 could promote the wound healing of both T1DM and T2DM mice (Fig. S3a, b).

In order to observe full wound closure in DM mice, we extended the time scale to 22 days. As shown in Supplementary Fig. S4, the skin wounds achieved their complete closure at day 18.0 ± 1.4 in T1DM mice, as compared to 12.0 ± 1.4 days in control counterparts. GDF11 treatment accelerated the full healing of diabetic skin wounds to day 15.0 ± 0.5.

Consistently, histological examination with Hematoxylin and Eosin (H&E) staining in T1DM wounds showed that granulation tissue deposition and new tissue formation were more abundant in wounds receiving topical rGDF11 at all time points examined than in mock-treated wounds (Fig. 1a).

Finally, we repeated the healing experiments by placing a silicone splint ring around the wounded area to prevent the possible confounding influence of wound contraction. As illustrated in Supplementary Fig. S5, GDF11 retained its ability to accelerate the healing of diabetic skin wound just as it did without the splint ring.

Neovascularization as a physiological mechanism for the DWH-promoting property of GDF11

Neovascularization is a key step for wound healing and this process is severely impaired in diabetes [31, 32]. Intriguingly, GDF11 has been documented to promote the cerebral vasculature through its pro-angiogenic property [16, 22]. These facts suggest that the DWH-promoting action of rGDF11 observed in our study is attributable to its pro-angiogenic property. To test this notion, we conducted the following experiments.

First, H&E staining demonstrated that the capillary density in the wound areas was substantially decreased in T1DM mice relative to healthy control counterparts, and such a decrease was pronouncedly rescued by rGDF11 (Fig. 1a). Additionally, the distance between epithelial tips was decreased, and the amount of granulation tissue was increased by GDF11 in the wound area of T1DM mice.

Second, we visualize the changes of neovascularization in wounded area treated with rGDF11 or vehicle in T1DM mice at day 7, by using immunostaining of an endothelial cell-specific marker CD31. Consistent with the H&E staining results, CD31 staining showed that the blood vessels in the dermal wound areas were rather scarce in T1DM mice than in healthy control animals (Fig. 1b). Yet, topical application of rGDF11 produced a robust increase in the number of blood vessels in diabetic wounds.

Masson staining showed that the collagen content of the granulation tissue was tremendously decreased on day 10 after creation of skin wound in non-treated T1DM mice, relative to that in non-T1DM control mice, and such a decline was reversed in T1DM mice treated with topical rGDF11 (50 ng/mL; Supplementary Fig. S6).

Next, histological examination by MicroPET/CT (Fig. 2a) and direct photographic examination of the wounded skin area (Fig. 2b), together with immunohistochemistry staining of CD31 (Supplementary Fig. S7), confirmed that T1DM reduced the number of neomicrovessels compared to the non-T1DM control group, whereas rGDF11 treatment (50 ng/mL) promoted neomicrovessels in T1DM mice. The angiogenic effect of rGDF11 was further confirmed by the chick chorioallantoic membrane (CAM) neovascularization assay. As depicted in Fig. 2c, the number of microvessels shown in the images and the relative number of vessels indicated by the statistical data were significantly increased by rGDF11 compared with non-treated and BSA-treated embryo chicks. Moreover, rGDF11 tremendously promoted the tube formation of HUVECs at the cellular level (Fig. 2d).

Cellular mechanism underlying the angiogenic potential of GDF11: the role of epithelial progenitor cells (EPCs)

Adult neovascularization occurs through two distinct processes: neovascularization (the sprouting of new blood vessels from preexisting ones) and vasculogenesis (the recruitment, proliferation, and assembly of bone marrow–derived endothelial progenitor cells EPCs into new vessels) [33]. EPCs are a cellular determinant of neovascularization because of their incorporation into the foci of neovascularization [34–36]. There is a possibility that GDF11 could impact EPCs in terms of their mobilization, migration and homing to wound site. Changes of the number of EPCs in blood reflect their mobilization from bone marrow and migration to the site of injury. We first identified EPCs as the $CD34^+/KDR^+/CD133^+$ cells from circulating mononuclear cell mix in the peripheral blood 5 days post-wounding and quantified the number of EPCs in the circulation. As illustrated in Supplementary Fig. S8, flow cytometry analysis revealed a marked decrease in EPC number in T1DM mice relative to control mice and a prominent restoration of circulating EPCs back to control levels in T1DM mice treated with rGDF11. (The control plot with unstained cells was provided in Supplementary Fig. S9a to demonstrate how the FACE gates were placed).

We next detected the number of EPCs in the lesions for EPC homing by immunofluorescent localization of $CD34^+/KDR^+$ cells (hematopoietic progenitor cell antigen and endothelial progenitor cell antigen, respectively). As depicted in Fig. 3a, the number of $CD34^+/KDR^+$ cells (or EPCs) was considerably lower in T1DM mice than in non-DM control counterparts. Treatment with rGDF11 abolished the DM-induced decrease in EPCs and restored the number back to the control level.

We subsequently investigated the effect of rGDF11 on trans-endothelial migration of EPCs by the Transwell method. The isolated EPCs were identified by dual staining with DiL-acLDL (red) and FITC-UEA-1 (green, Supplementary Fig. S10). As shown in Fig. 3b, rGDF11 pronouncedly enhanced the ability of EPCs to migrate, relative to non-treated cells.

We further studied the effect of rGDF11 on tube formation using Matrigel assay. As demonstrated in Fig. 3c, compared with non-treated control cells, the EPCs treated with rGDF11 had larger tube areas and longer tube length.

These data indicate that GDF11 promotes the wound healing and neovascularization mainly through increasing the mobilization, migration, homing, and tube formation of EPCs at the cellular level.

Molecular mechanisms underlying the angiogenic potential of GDF11: the role of HIF-1α signaling

Hypoxia-inducible factor-1 alpha (HIF-1α), a master transcription factor, is critically involved in virtually all processes of wound healing and vascular remodeling [37]. Impaired functionality of HIF-1α can hamper neovascularization. HIF-1α is a key factor in regulating transcription of VEGF, a crucial protein that stimulates EPC mobilization from bone marrow and migration to lesion site through upregulating expression of stromal cell-derived factor-1α (SDF-1α) [38–40]. EPC recruitment to the wound site depends on upregulation of SDF-1α and decrease in SDF-1α can retard EPC homing. These facts urged us to investigate if the increased EPC migration and homing in rGDF11-treated DM mice was associated with altered levels and/or activities of the above-mentioned factors. Our data indeed showed that on day 5 after wound creation the mRNA levels of HIF-1α, VEGF, and SDF-1α were all significantly upregulated by rGDF11 (Fig. 4a). Consistently, protein levels of HIF-1α, VEGF, and SDF-1α were also robustly elevated in

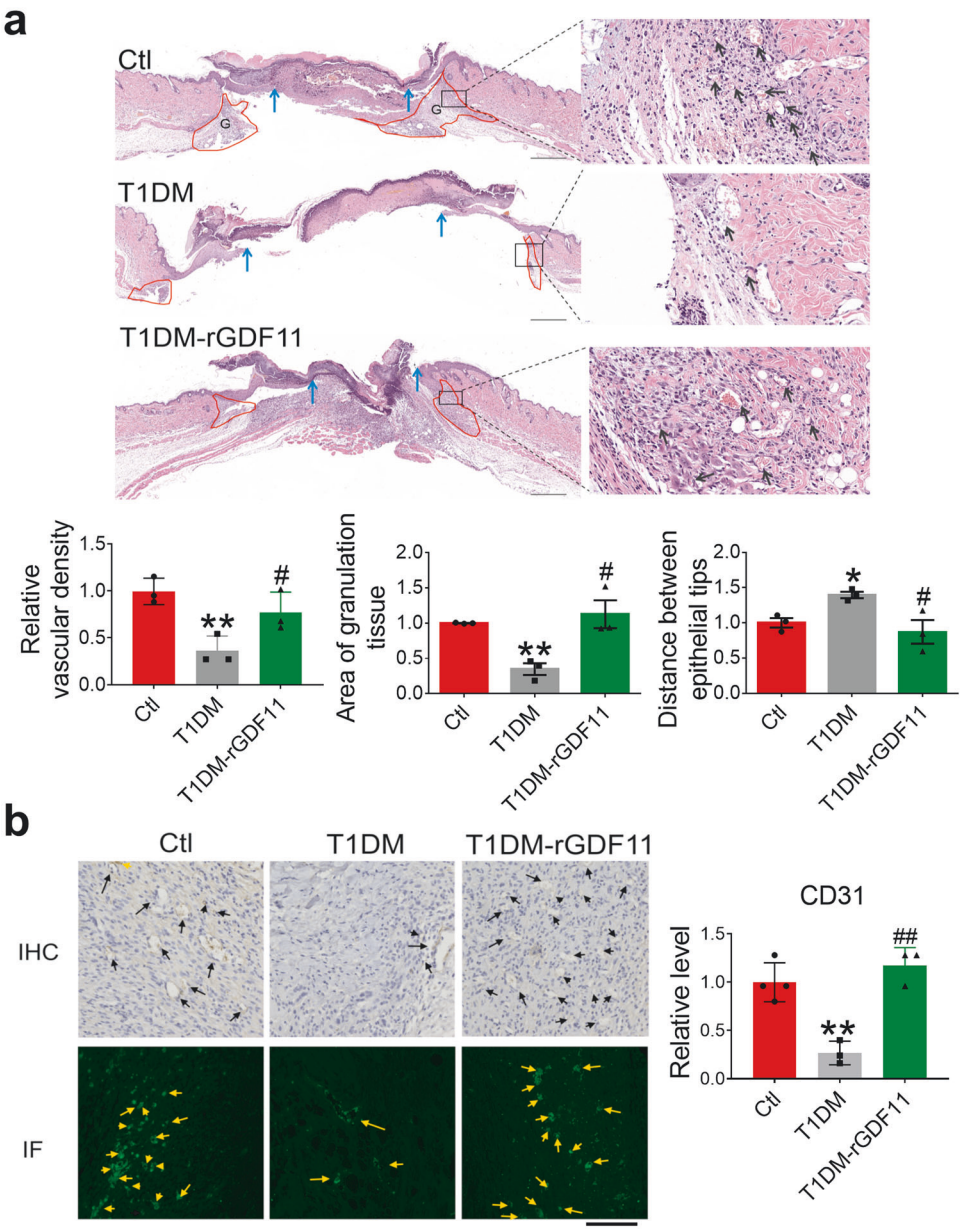

Fig. 1 GDF11 induces neovascularization in diabetic wounds as revealed by histopathological analyses in STZ-induced T1DM mice. **a** Typical examples of hematoxylin and eosin (H&E) staining showing the enhanced granulation tissue deposition (indicated by vessels, fibers and inflammatory cells) and neovascularization (black arrows in the right panels), and simultaneously decreased distance between epithelial tips (as indicated by the shortened distance between the blue arrows) induced by topical administration of rGDF11 (50 ng/mL) in the wounded skin area on day 5 following wound creation. Note the increased number of vessels with rGDF11 treatment, as indicated by red circular structures pointed by dark arrows. The distance between epithelial tips was defined by blue arrows, and area of granulation was outlined by red lines and labeled with "G". Magnification: ×30 for left panels and 365× for right panels. Similar results were consistently observed in another two groups of animals. $^{*}P < 0.05$, $^{**}P < 0.01$ *vs.* Ctl; $^{\#}P < 0.05$, *vs.* T1DM; $n = 3$. **b** Typical examples of CD31 staining showing the enhanced neovascularization induced by topical administration of rGDF11 (50 ng/mL) in the wounded skin area on day 7 following wound creation. Note the increased number of vessels following rGDF11 treatment, as indicated by brown circular structures pointed by dark (upper panels) and yellow (lower panels) arrows. Magnification: ×200. Similar results were consistently observed in another two experiments. $^{**}P < 0.01$ *vs.* Ctl; $^{\#\#}P < 0.01$ *vs.* T1DM; $n = 3$–4. (Mean ± SEM; ANOVA followed by Dunnett's test for comparisons among multiple groups, and Student's *t*-test for comparisons between two groups).

the wounded area of rGDF11-treated T1DM mice relative to non-treated T1DM mice (Fig. 4b).

To verify the role of HIF-1α in mediating the DWH-promoting action of rGDF11, we took the advantage of HIF-1α inhibitor PX-478 as a pharmacological tool in the subsequent experiments. As illustrated in Fig. 5a, rGDF11 lost its ability to promote DWH in T1DM mice pretreated with PX-478 (20 μM). To better understand the role of HIF-1α inhibitor PX-478 alone on wound healing, we performed the diabetic wound healing assay. As shown in Supplementary Fig. S11, the diabetic wound healing was slower than Ctl mice. The inhibition of HIF-1α prolongs the diabetic wound healing process. Immunofluorescence staining of $CD34^{+}$/KDR^{+} cells indicated that the number of EPC homing to wound site was also significantly decreased after inhibition of HIF-1α (Fig. 5b). To better illustrate the dynamic changes in EPC migration and homing, we performed the flow cytometry of wounded skin

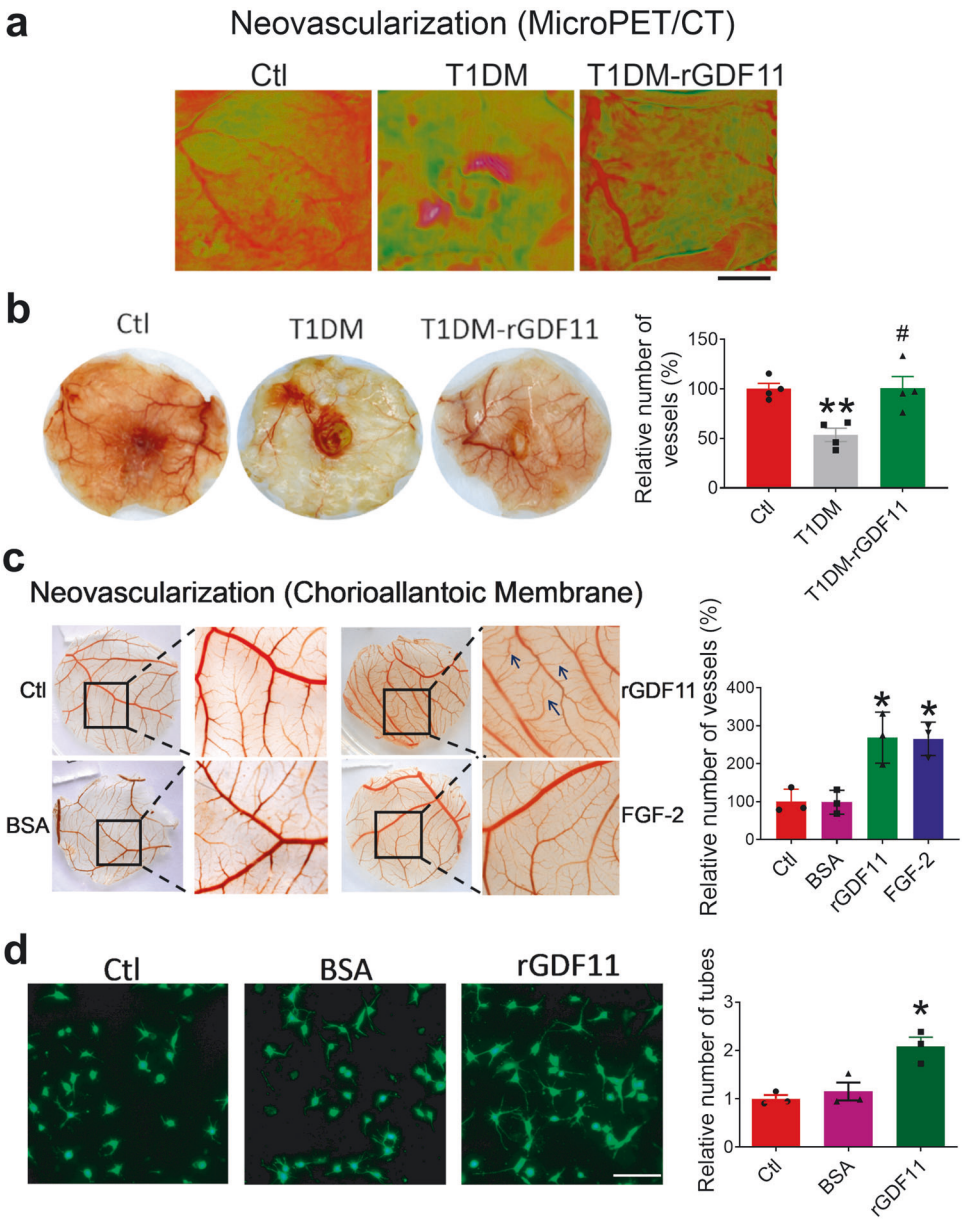

Fig. 2 DF11 induces neovascularization in diabetic wounds as revealed by MicroPET/CT analysis and chick embryo chorioallantoic membrane (CAM) assay in STZ-induced T1DM mice. a, **b** Representative MicroPET/CT images and photographs of the wounded skin area (day 7) showing the enhanced neovascularization induced by topical application of rGDF11 (50 ng/mL). Note the markedly increased number of vessels with rGDF11 treatment. $^{**}P < 0.01$ *vs*. Ctl, $^{\#}P < 0.05$ *vs*. T1DM; $n = 4$. **c** Left panel: typical examples of the chick embryo chorioallantoic membrane (CAM) examination showing the enhanced neovascularization induced by topical administration of rGDF11 (50 ng/mL) in the wounded skin area; right panel: averaged relative blood vessel density. $^{*}P < 0.05$ *vs*. Ctl or BSA; $n = 3$. **d** Left panel: Representative images (×100 magnification) showing the effect of rGDF11 (50 ng/mL; incubation for 24 h) on the tube formation in HUVEC cells with Matrigel assay; right panel: statistical data on the relative number of tubes quantified using ImageJ software. $^{*}P < 0.05$ *vs*. Ctl or BSA; $n = 3$. (Mean ± SEM; ANOVA followed by Dunnett's test for comparisons among multiple groups, and Student's *t*-test for comparisons between two groups).

on Day 5. As shown in Fig. 5c, the EPCs, marked with CD133 & CD34 & CD309 (KDR) were decreased in diabetic wounded skin. After rGDF11 administration, the number of EPCs was elevated significantly. The inhibition of HIF-1α by PX-478 could partially alleviate the mobilization of EPC by rGDF11 (Fig. 5c). The flow cytometry analysis also demonstrated that the EPC mobilization from bone marrow to circulation was decreased in the presence of PX-478 compared with the rGDF11 group (Supplementary Fig. S8). Moreover, the vessel density was considerably reduced by PX-478 (Fig. 5d). Similar to the above in vivo data, rGDF11 failed to promote the migration and tube formation of EPCs after PX-478 treatment under in vitro conditions (Fig. 5e, f).

GDF11 is downregulated in diabetic skin wounds

The data presented above have clearly demonstrated the efficacy of rGDF11 and the cellular and molecular mechanisms in DWH. We next sought to clarify whether GDF11 is merely an agent that could be applied to diabetic skin wound or is also a causal factor for the non-healing nature of diabetic wounds. We first investigated whether expression of endogenous GDF11 (eGDF11) was affected by T1DM. To this end, we measured the changes of eGDF11 mRNA and protein levels around the wounded area. As shown in Fig. 6a, b (left), substantial decreases in eGDF11 expression at both mRNA and protein levels were consistently observed in diabetic skin wounds.

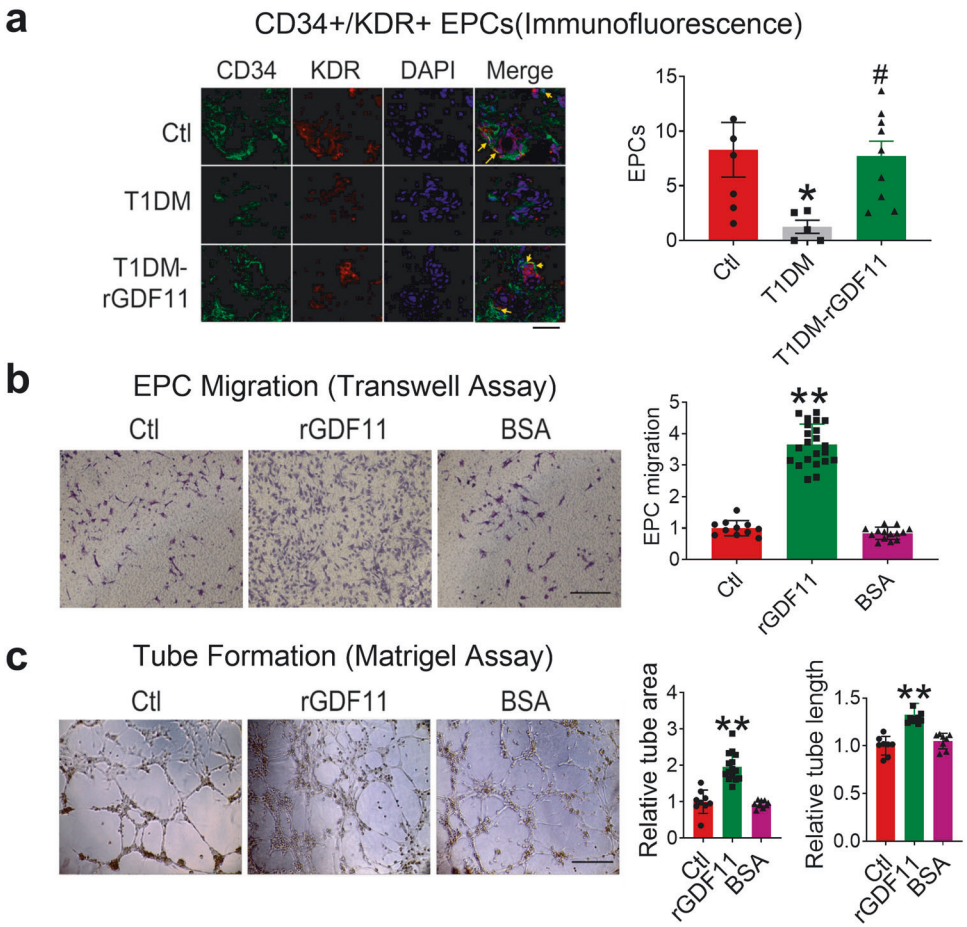

Fig. 3 GDF11 promotes mobilization, migration and homing of epithelial progenitor cells (EPCs) and tube formation. a Immunofluorescent localization (left panel; magnification ×600) and quantification (right panel) of $CD34^+/KDR^+$ EPCs (mean intensities from merged signals) in the wounded area (the fifth day after creation of a dermal wound) as an indication of EPC homing to the lesion. Shown are the ratios of EPCs over total cells. Note that the number of $CD34^+/KDR^+$ cells was considerably lower in T1DM mice than in non-DM control counterparts and treatment with rGDF11 restored the number of EPCs in the wounded area. $^*P < 0.05$ *vs.* Ctl, $^{\#}P < 0.05$ *vs.* T1DM; $n = 5$–9 for each group. **b** Transwell assay for the effect of rGDF11 on migration of EPCs isolated from healthy mice. Note that the ability of EPC migration was substantially enhanced by rGDF11. BSA was used as a vehicle control. Magnification: ×100. $^{**}P < 0.01$ *vs.* Ctl or BSA; $n = 11$–22 for each group. **c** Matrigel assay for the effect of rGDF11 on tube formation of EPCs. Compared with the control groups, rGDF11-treated cells exhibited larger tube area and longer tube length. Magnification: ×100. $^{**}P < 0.01$ *vs.* Ctl or BSA; $n = 8$–15. (Mean ± SEM; ANOVA followed by Dunnett's test for comparisons among multiple groups, and Student's *t*-test for comparisons between two groups).

The specificity of the GDF11 antibody used in our study was verified using the purified recombinant GDF11 and GDF8. As shown in Fig. 6b (right), the GDF11 antibody recognized only rGDF11 and no cross-reaction with GDF8 was observed.

Downregulation of GDF11 delays the healing process of diabetic skin wounds

We then asked ourselves whether downregulation of eGDF11 is merely a bystander of the pathological process of diabetic wounds, a consequence to diabetes or skin damage, or a causal factor for the non-healing nature of diabetic wounds. To clarify this issue, we employed loss-of-function approaches to see if artificial inhibition of GDF11 function and silence of GDF11 expression could mimic the effects of DM on wound healing. We examined the effects of GDF11 antibody (anti-GDF11) on wound healing in otherwise healthy mice and consistently observed that anti-GDF11 reproduced the same delaying effects of wound healing as seen in DM mice (Fig. 6c). Specifically, anti-GDF11 increased the healing time course with a duration spanning 50% wound closure (WCT50) value to 7.6 days from the control value of 4.6 days. As a negative control IgG antibody did not produce any appreciable effect on the wound-healing process. To better understand the effects of anti-GDF11 on wound healing in diabetic mice, we performed the diabetic wound healing assay. As shown in Supplementary Fig. S12, anti-GDF11 prolonged the diabetic wound healing process.The efficacy of the antibody in suppressing GDF11 function was confirmed by the data showing a loss of the ability of GDF11 to activate Smad2/3 as reflected by the decreased level of p-Smad2/3 (Fig. 6d).

Active GDF11 is 89% identical to GDF8 (myostatin, a muscle growth factor) in their amino acid sequences. To clarify if the healing-promoting effect observed in our experiments was primarily afforded by GDF11, but not by GDF8, we detected the wound healing after topical injection of AAV8 virus containing the small guide RNA directed to GDF11 (AAV8-sgGDF11). AAV8-sgGDF11 silenced the expression of GDF11 as indicated by the decreased GDF11 mRNA level but did not influence the expression of GDF8 (Supplementary Fig. S13). The specific silencing of GDF11 delayed the healing process (Fig. 7a). Silence of GDF11 increased the WCT50 to 5.9 days in T1DM mice from 4.0 days in control littermates. The negative control virus (sgNC) had no effect on wound healing (Fig. 7a). Similar wound healing-retarding effect of GDF11 inhibition was seen under in vitro conditions with GDF11 siRNA (siGDF11) to silence the expression of eGDF11 (Fig. 7b–d). As depicted in Fig. 7b, siGDF11 resulted in

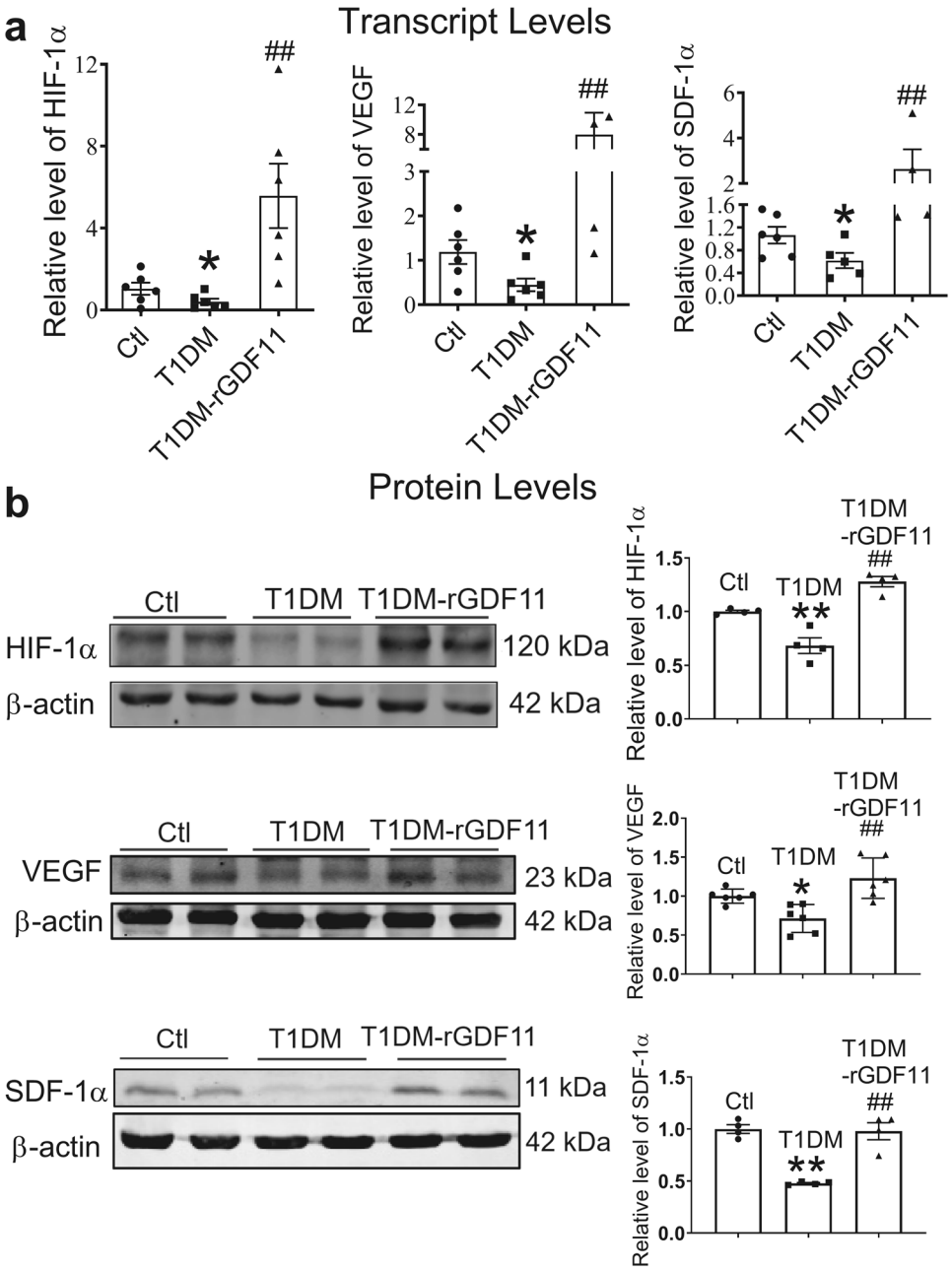

Fig. 4 Abnormal downregulation of neovascularization-related genes/proteins HIF-1α, VEGF, and SDF-1α, and restoration of their expression by GDF11. a Expression downregulation of mRNA levels of HIF-1α, VEGF, and SDF-1α in the wounds of T1DM mice and restoration of their expression by rGDF11. $^{*}P < 0.05$ *vs*. Ctl, $^{\#\#}P < 0.01$ *vs*. T1DM; $n = 4$–6 for each group. **b** Expression downregulation of protein levels of HIF-1α, VEGF, and SDF-1α in the wounds of T1DM mice and restoration of their expression by rGDF11. $^{*}P < 0.05$ & $^{**}P < 0.01$ *vs*. Ctl, $^{\#\#}P < 0.01$ *vs*. T1DM; $n = 4$–6 for each group. (Mean ± SEM; ANOVA followed by Dunnett's test for comparisons among multiple groups, and Student's *t*-test for comparisons between two groups).

pronounced decreases in the expression of HIF-1α and VEGF at both mRNA and protein levels in HUVECs. As anticipated, migration and tube-forming ability of EPCs were also markedly weakened in the presence of siGDF11 in EPCs isolated from healthy mice (Fig. 7c, d).

The ability of siGDF11 to silence eGDF11 was verified (Supplementary Fig. S13c). By comparison, sgNC and siNC (a negative control siRNA construct) failed to elicit any meaningful effects on the expression of eGDF11, HIF-1α and VEGF, and on the function of EPCs either (Fig. 7a–d).

On the other hand, when GDF8 was specifically silenced by AAV8-sgGDF8, application of rGDF11 remained its effectiveness in accelerating wound healing in T1DM mice (Supplementary Fig. S14).

DISCUSSION

The non-healing nature of diabetic wounds has been a persistent clinical problem even though we have witnessed rapidly emerging modern biomedical technologies and revolving therapeutic conceptions and approaches. The aims of the present study were to investigate the role of GDF11 in controlling the healing of diabetic skin wound and to elucidate the underlying mechanisms. Our data demonstrated that topical

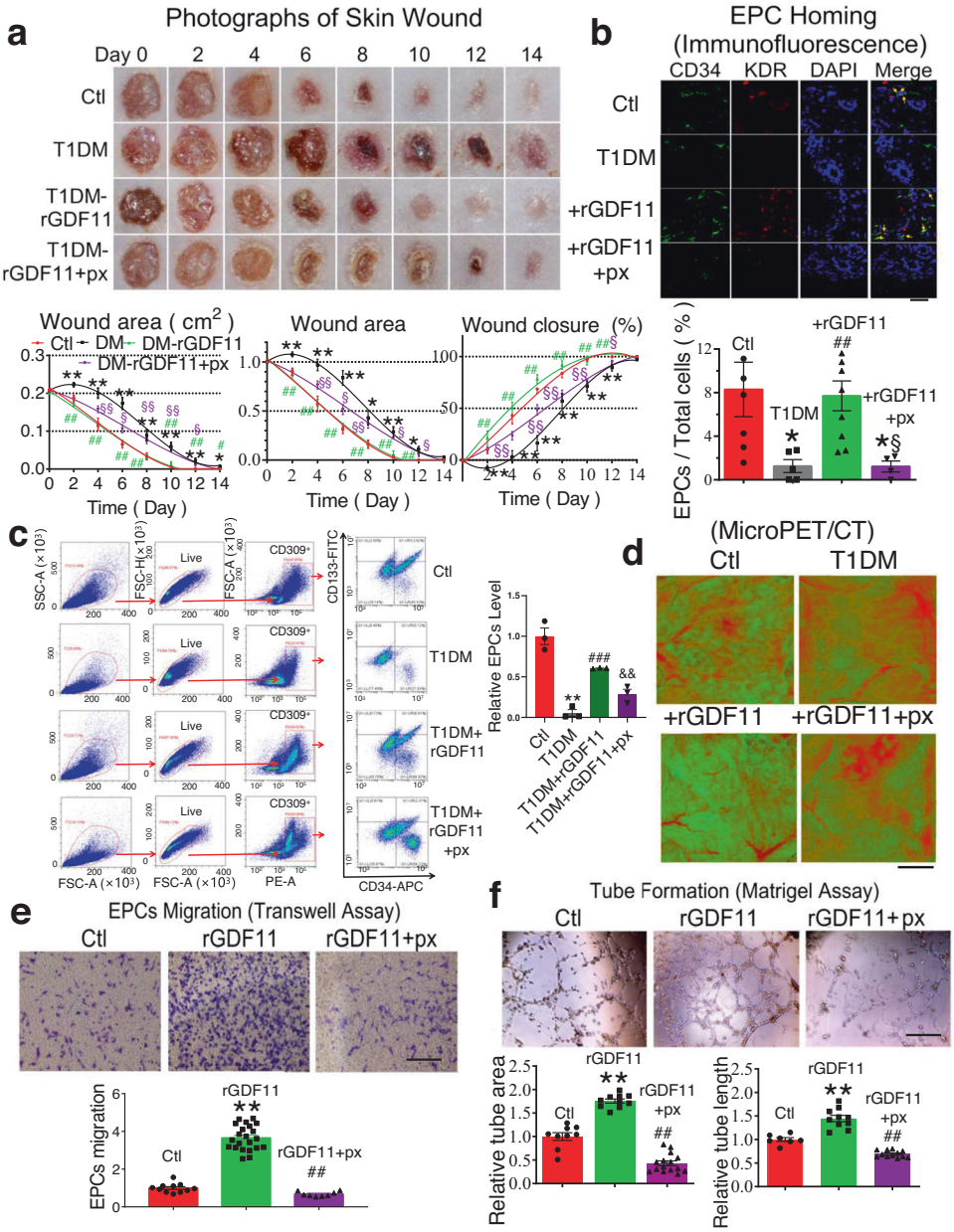

Fig. 5 Verification of the role of HIF-1α in mediating the diabetic wound healing-promoting action of GDF11. a Photographs and mean data of dermal wounds showing the counteracting action of HIF-1α inhibitor PX-478 (20 μM; px) to the accelerating effects of GDF11 on wound healing. $^{*}P < 0.05$ & $^{**}P < 0.01$ *vs.* Ctl; $^{\#}P < 0.05$ & $^{\#\#}P < 0.01$ *vs.* T1DM; $^{\S}P < 0.05$ & $^{\S\S}P < 0.01$ *vs.* T1DM-rGDF11; $n = 5$–7 for each group. **b** Immunofluorescence staining of EPCs showing the counteracting action of HIF-1α inhibitor PX-478 (px) to the promoting effects of GDF11 on EPC homing to the lesion. Mean data from the merged signals are expressed as the ratios of EPCs over total cells. Magnification: ×600. $^{*}P < 0.05$ *vs.* Ctl, $^{\#\#}P < 0.01$ *vs.* T1DM, $^{\S}P < 0.05$ *vs.* T1DM-rGDF11; $n = 5$–9 for each group. **c** Flow cytometry analysis demonstrating the counteracting action of HIF-1α inhibitor PX-478 (px) to the enhancing effects of GDF11 on EPC homing of wounded skin in day 5. $^{**}P < 0.01$ vs. Ctl, $^{\#\#\#}P < 0.001$ vs. T1DM, $^{\&\&}P < 0.05$ vs. T1DM + rGDF11; $n = 3$ for each group. **d** MicroPET/CT images of the skin wound depicting the counteracting action of HIF-1α inhibitor PX-478 (20 μM; px) to the beneficial effects of GDF11 on the growth of vessels. **e** Transwell assay demonstrating the counteracting action of HIF-1α inhibitor PX-478 (px) to the enhancing effects of GDF11 on EPC migration. Magnification: ×100. $^{**}P < 0.01$ *vs.* Ctl, $^{\#\#}P < 0.01$ *vs.* T1DM; $n = 8$–22 for each group. **f** Matrigel assay demonstrating the counteracting action of HIF-1α inhibitor PX-478 (px) to the enhancing effects of GDF11 on tube formation. Magnification: ×100. $^{**}P < 0.01$ *vs.* Ctl, $^{\#\#}P < 0.01$ *vs.* T1DM; $n = 7$–12 for each group. (Mean ± SEM; ANOVA followed by Dunnett's test for comparisons among multiple groups, and Student's *t*-test for comparisons between two groups).

application of rGDF11 effectively accelerated the healing processes of full-thickness cutaneous wounds in the settings of both Type 1 and Type 2 diabetes mellitus (T1DM and T2DM). We also presented the evidence for the downregulation of eGDF11 as a critical cause for the non-healing nature of diabetic wounds. The wound healing-promoting properties of rGDF11 could be ascribed to its ability to enhance neovascularization through mobilizing EPCs and upregulating HIF-1α to enhance the activities of VEGF and SDF-1α at the cellular and molecular levels, respectively. Our study has therefore uncovered a novel mechanism of GDF11 in promoting diabetic wound healing that is GDF11 stimulates endothelial progenitor cells mobilization and accelerates neovascularization mediated by HIF-1α-VEGF/SDF-1α pathway.

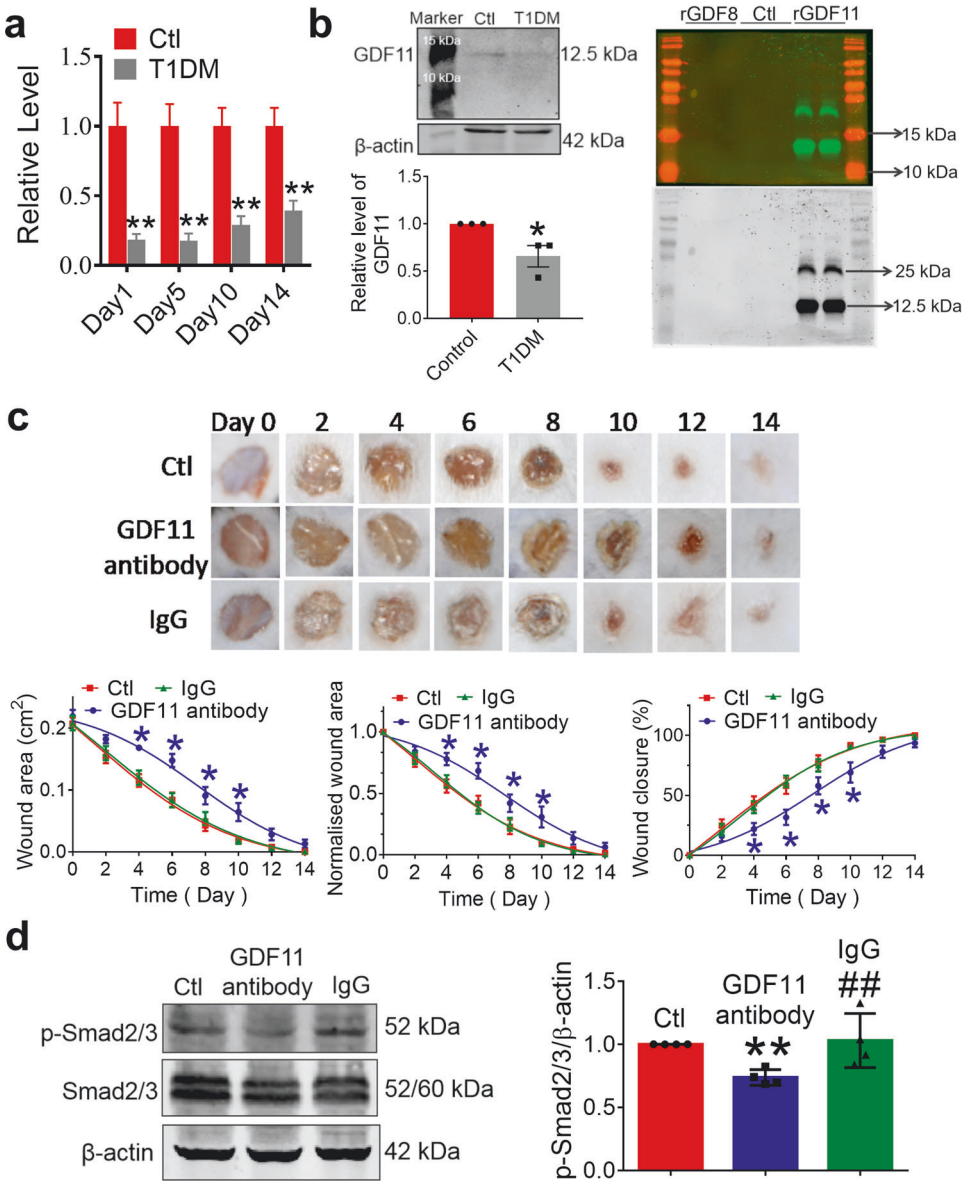

Fig. 6 Downregulation of GDF11 in diabetic skin wounds delays the healing process. a Downregulation of endogenous GDF11 (eGDF11) at the mRNA level around the wounded area of T1DM mice relative to non-DM control mice from day 1 to day 14 after creation of skin wound. $^{**}P < 0.01$ *vs.* non-DM control; $n = 8$–11 for each group. **b** Downregulation of endogenous GDF11 (eGDF11) at the protein level around the wounded area of T1DM mice. Left panel:.Western blot results. Right panel: verification of specificity of the anti-GDF11 antibody using the purified recombinant GDF11 and GDF8. No cross-reaction was noted between GDF11 and GDF8; that is, the anti-GDF11 antibody recognized only rGDF11 without picking up GDF8. $^{*}P < 0.05$ *vs.* control; $n = 3$ for each group. **c** Upper panel: representative photographs showing the time-dependent closure of wounds in otherwise healthy and the wound healing-retarding effect of GDF11 antibody. Lower left panel: averaged raw values of remaining wound area as a function of time (day). Lower middle panel: averaged normalized values of remaining wound area as a function of time (day). The data collected at varying time points were normalized to those at 0 time point. Lower right panel: averaged values of wound closure as a function of time (day), expressed as percentage of wound closure. $^{*}P < 0.05$ *vs.* Ctl; $n = 6$–12 for each group. **d** Verification of the efficacy of GDF11 antibody in inhibiting GDF11 function as indicated by the failure of Smad2/3 activation (decreases in p-Smad/2/3) in HUVECs. $^{**}P < 0.01$ *vs.* Ctl, $^{\#\#}P < 0.01$ *vs.* rGDF11; $n = 4$ for each group. (Mean ± SEM; ANOVA followed by Dunnett's test for comparisons among multiple groups, and Student's *t*-test for comparisons between two groups).

Previous studies on GDF11 functionalities

GDF11, a member of the transforming growth factor-β superfamily of secreted factors, is known for its critical participation in the regulation of cell growth and differentiation in both embryonic and adult tissues. Relevant to the present study, there are original researches linking GDF11 to pancreatic islet function thereby diabetes. Harmon et al. [41] demonstrated that GDF11 null mice have profound defects in pancreatic islet development, leading to increased number of islet progenitors but impaired maturation of β-cells, an overall reduction in β-cell mass, and an increased α-cell mass in mutants compared to newborns of wild-type GDF11. In line with this finding, Li et al. [42] further unraveled that systematic replenishment of GDF11 not only preserves insulin secretion but also improves the survival and morphology of β-cells in both nongenetic and genetic mouse models of T2DM through the activation of the TGF-β/Smad2 and PI3K-AKT-FoxO1 signaling pathways. Nevertheless, despite the general interest in GDF11 research, our group firstly reported the potential involvement of GDF11 in skin tissue repair [27]. Topical application of GDF11 pronouncedly expedited diabetic skin wound healing in mice models of both STZ-induced T1DM and

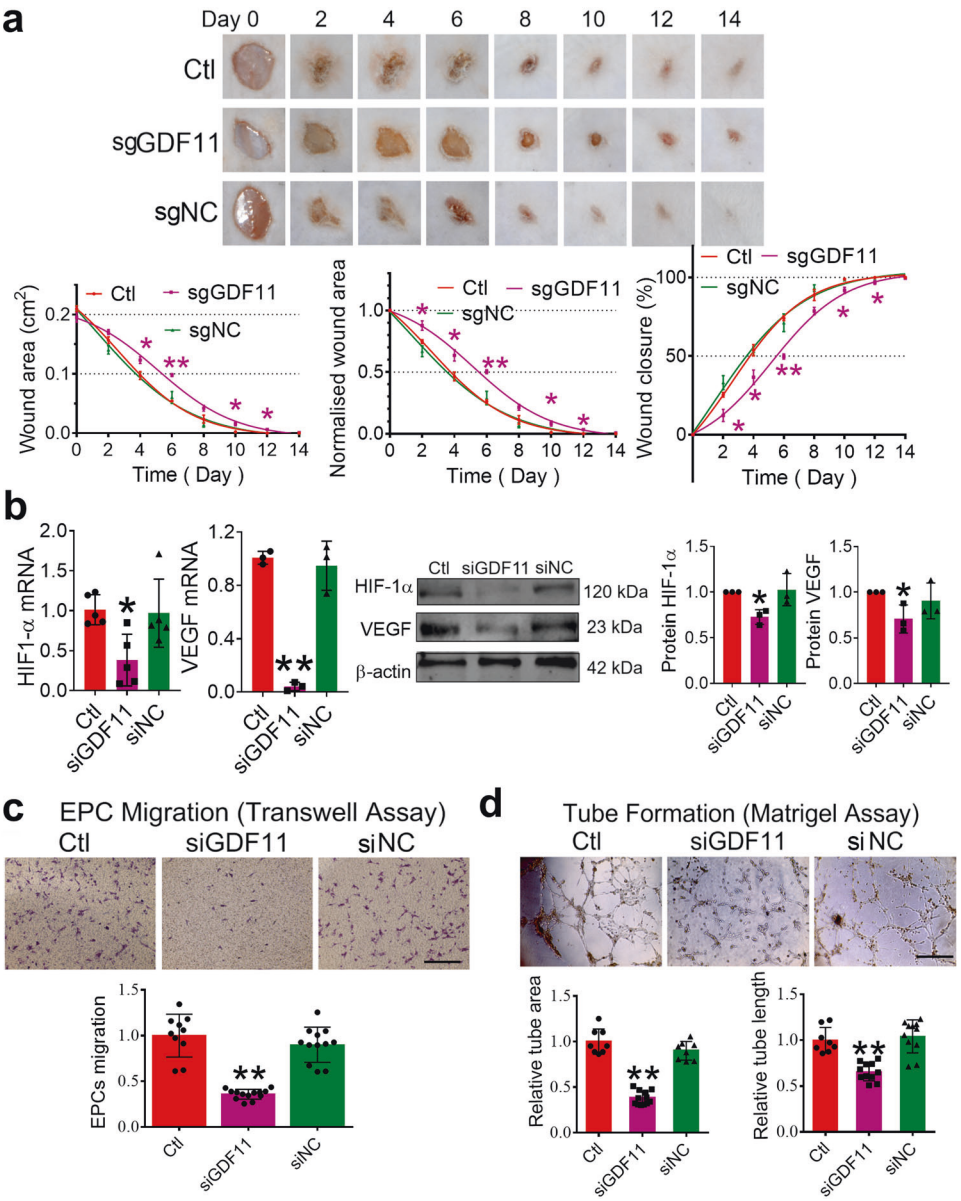

Fig. 7 Downregulation of GDF11 in diabetic skin wounds delays the healing process. a Upper panels: representative photographs showing the time-dependent closure of wounds in otherwise healthy mice and the wound healing-retarding effect upon silencing GDF11 by AAV8-sgGDF11 ("sg" represents small guide RNA for silencing GDF11 expression). Lower panels: averaged raw values of remaining wound area as a function of time (day; left panels); averaged normalized values of remaining wound area as a function of time (day; middle panel). The data collected at varying time points were normalized to those at 0 time point; averaged values of wound closure as a function of time (day; right panels), expressed as percentage of wound closure. $^{*}P < 0.05$ & $^{**}P < 0.01$ *vs.* Ctl; $n = 4$ for each group. **b** Silencing of eGDF11 reduced the mRNA (left) levels of HIF-1α and VEGF in HUVECs (left two panels). $^{*}P < 0.05$ & $^{**}P < 0.01$ *vs.* Ctl & NC (siNC); $n = 3$–5 for each group. Silencing of eGDF11 reduced the protein (right) levels of HIF-1α and VEGF in HUVECs (right two panels). $^{*}P < 0.05$ *vs.* Ctl & NC (siNC); $n = 3$ for each group. **c** Silencing of eGDF11 weakened the ability of migration of EPCs isolated from healthy mice, as revealed by Transwell assay. Magnification: ×100. $^{**}P < 0.01$ *vs.* Ctl & NC (siNC); $n = 10$–13 for each group. **d** Silencing of eGDF11 weakened tube formation of EPCs isolated from healthy mice, as revealed by Matrigel assay. Magnification: ×100. $^{**}P < 0.01$ *vs.* Ctl & NC (siNC); $n = 8$–12 for each group. (Mean ± SEM; ANOVA followed by Dunnett's test for comparisons among multiple groups, and Student's *t*-test for comparisons between two groups).

Lepr$^{db/db}$ T2DM [27]. It is worth mentioning that the GDF11 protein synthesized in our own laboratory produced nearly identical actions with compatible potencies to the commercially purchased GDF11 [27], which excluded the potential variations due to different sources of GDF11. What's more, GDF11 also has a certain promoting effect on the wound healing of non-diabetic mice. This work has been published in Chinese Invention Patents (authorized, NO. ZL20160150511.0). This finding indicates that GDF11 could reverse the loss of healing capability and capacity upon administration to the site of trauma.

Probably equally important is our finding that endogenous GDF11 was considerably downregulated around the wounded areas of diabetic mice, and inhibition of eGDF11 function or silence of eGDF11 expression retarded the healing process of diabetic skin wound and reduced neovascularization, for these observations suggest that GDF11 might be one of the causal factors for the non-healing nature of diabetic wounds. This finding also explains from a different angle why exogenously supplied GDF11 or GDF11 replacement is effective in battling against the difficulty of wound healing in diabetes. It is worthy of mentioning

that the employment of GDF11-specific antibody for verifying the beneficial action of GDF11 both in vivo and in vitro should have strengthened our observations and conclusions.

Mechanisms for the beneficial actions of GDF11

Diabetic dermal wounds are deficient in angiogenic and vasculogenic processes, and such deficiencies are characterized by, and likely due to, a reduced level of some key growth factors [36]. In the efforts to decipher the underlying mechanisms for the efficacy of rGDF11 in promoting the process of diabetic skin wound healing (DWH), we have obtained the data at three levels as discussed below.

At the physiological level, vascular endothelial dysfunction is known to predispose diabetic patients to numerous cardiovascular complications, including delayed wound healing. Attenuated angiogenic response to tissue injury and hypoxia in diabetes likely contribute to the strong propensity to develop persistent decubitus and foot ulcers [43, 44]. Our data unraveled that the DWH-promoting property of rGDF11 could likely be ascribed to its ability to reactivate the processes of neovascularization. Four lines of evidence were presented in the present study. (1) H&E staining of wound tissue demonstrated that rGDF11 increased the capillary density in the wound areas of DM mice. (2) Immunostaining of CD31 of lesion sections showed the prominently enhanced neovascularization both at the margin of wound and endocentrically within the wounds treated with rGDF11. (3) MicroPET/CT scanning of lesions revealed that GDF11 treatment robustly accelerated the growth of neomicrovessels. (4) Our neovascularization assay using the chick chorioallantoic membrane further exhibited the significantly increased microvessels by rGDF11, confirming the vasculogenic potential of GDF11. It is interesting to note that in both T1DM and T2DM mice, the wound area was enlarged within the first three days after creation of the lesions, as clearly shown by the initial increasing phase in the wound-area curves or the initial decreasing phase in the wound-closure curves. Yet, such DM-induced worsening of wound was eliminated in the mice treated with rGDF11. The role of GDF11 in neovascularization has been reported in cerebral vasculature related to neurogenesis and olfactory discrimination [16] and in the border zone of ischemic heart of both young and old mice with increased capillary and arteriolar densities [22]. In addition, it has also been shown that GDF11 treatment enhances in vitro sprout formation with capillary-like sprouts originating from the central plain of EPC individual spheroids ref. 23. However, whether GDF11 also promotes neovascularization in the dermal tissues remained unstudied previously. Our study therefore represents the first to identify and characterize the ability of GDF11 to enhance dermal neovascularization. Especially in the setting of DM with neovascularization being severely impaired, the strong promoting properties of GDF11 are exceptionally promising.

At the cellular level, the processes of neovascularization require an elaborate cascade of signaling events capable of mobilizing, homing, and retaining EPCs [45]. In other words, wound healing relies on the mobilization of EPCs from the bone marrow and trafficking to site of tissue regenerating or wound healing. During the process of wound healing in non-diabetic subjects, EPCs are effectively recruited to the site of trauma, leading to wound revascularization thereby timely healing. Such a response however is dampened in diabetic ulceration [46]. In our study, GDF11 strongly promoted the mobilization, migration and homing of EPCs to the site of dorsal skin wounds, as supported by the follow cytometry analysis showing the increased number of circulating EPCs, transwell assay showing the enhanced transendothelial migration of EPCs, and immunofluorescent localization showing the increased distribution of EPCs in the site of lesion. Similar properties of GDF11 have been documented in the literature. For example, one study reported that GDF11 supports migration and sprouting of endothelial progenitor cells [23]. Together our findings and the published data, it is clear that the favorable regulatory role of GDF11 in EPC function is the primary cellular mechanism for its efficacy in neovascularization.

At the molecular level, it is known that wound healing is a complex multi-step process that requires spatial and temporal orchestration of cellular and non-cellular components, among which the master transcription factor HIF-1α plays a key role in neovascularization by activating the expression and stimulating the secretion of VEGF and SDF-1α in macrophages and fibroblasts [47–49]. Recently, it has been reported that increased polyubiquitinated degradation of HIF-1α in diabetic wounds impairs the efficacy of wound healing [50]. VEGF serves to activate EPCs from the bone marrow to the peripheral circulation [39, 51] and SDF-1α to induce migration and recruitment of EPCs to the damaged area [52–54]. The blunted neovascularization in diabetic wounds is largely caused by decreased levels of VEGF and SDF-1α [45, 52]. Our experiments generated the data exhibiting the positive regulatory effects of GDF11 on the expression of HIF-1α, VEGF, and SDF-1α at both mRNA and protein levels in the lesion site of diabetic mice. Silencing of eGDF11 decreased the expression of these factors. More conclusively, in the presence of HIF-1α inhibitor PX-478, GDF11 lost its ability to promote mobilization, migration, homing and tube formation of EPCs with a consequent loss of neovascularization thereby of diabetic wound healing. The results strongly support HIF-1α as a mechanistic link between GDF11 and wound healing. In addition to the HIF-1α-VEGF/SDF-1α signaling pathway, the TGF-β-Smad2/Smad3 pathway might also participate in the GDF11-induced EPC migration, as one study described that treatment of EPCs with rGDF11 results in activation of the Smad2/Smad3 pathway along with an increase in migration, which can be inhibited by the TGF-β1 superfamily type-I activin receptor-like kinase inhibitor SB431542 [55]. Moreover, our previous research showed that GDF11 could promote /accelerate the healing process of skin wound in mice of diabetes by stimulating dermal fibrosis via the YAP/Smad2/3/CTGF signaling pathway [27]. Furthermore, GDF11 may improve the diabetic wound through anti-inflammation pathway, as Wang et al. demonstrated that GDF11 could antagonize psoriasis-like skin inflammation via suppression of NF-κB signaling pathway [56].

Taken together, it is reasonable to propose the following sequence of events for the wound healing-facilitating property of GDF11. (1) Endogenous GDF11 is downregulated in the diabetic lesion rendering the non-healing nature of diabetic wounds; (2) Topical application of exogenous rGDF11 upregulates HIF-1α that then stimulates expression and secretion of VEGF and SDF-1α; (3) Increases in VEGF and SDF-1α in turn promote the activation and migration of EPCs from the bone marrow and destines to the lesion area; (4) Mobilization and homing of EPCs then enhance neovascularization; and (5) The above steps finally conduce the healing of diabetic wounds.

Possible limitations of this study

It should be noted that there are several limitations in the present study. First, we have not elaborated the mechanisms by which GDF11 enhanced expression of HIF-1α. Given the fact that GDF11 upregulated the mRNA level of HIF-1α, it is possible that GDF11 directly or indirectly activates transcription of this gene. To clarify this issue, we did some prediction work and found that GDF11 may regulate the expression of HIF1α via activating SMAD2/3/4 heteromers to promote the transcription of HIF1α. And preliminary results showed that GDF11 could promote HIF-1α to enter the nucleus. Yet, further studies are absolutely required to clarify this issue. Second, it remains presently unclear how topical application of GDF11 could mobilize EPCs supposedly from bone marrow. One possible explanation is that GDF11 boosted up expression and secretion of VEGF into circulation where the latter travels to bone marrow and take its actions. In support of this notion, numerous studies have shown that VEGF produced in the site of tissue injury can stimulate mobilization of EPCs in bone marrow [57, 58]. Third,

our data were acquired from mouse models and the results may not be readily applicable to humans and thus the clinical implications are still uncertain at this stage. Nevertheless, we used human recombinant GDF11 in our study and the mouse models of diabetes used in our study have been widely employed for pharmacological investigations. In this sense, our findings should bear a relevance to the dermal wounds in patients with diabetes.

In summary, the present study generated a number of novel findings. First, our study identified GDF11 as a new agent that can facilitate neovascularization to help skin tissue regeneration and regain the lost capability and capacity of wound healing in the setting of diabetes. Second, our data suggest that deficiency of GDF11 is a new factor accounting partially for the non-healing nature of diabetic wounds. Third, GDF11 stimulated HIF-1α to regain the lost ability of neovascularization leading to facilitation of diabetic wound healing. These findings help us better understand the pathophysiological and molecular mechanisms of GDF11 function and the associated non-healing feature of diabetic wound and suggest GDF11 as a potential new agent for the clinical treatment of diabetic skin wound.

ACKNOWLEDGEMENTS

This work was supported in part by the grants from National Key R&D Program of China (2017YFC1307403), the National Natural Science Foundation of China (81730012, 91949130, 81970320, 82003749 and 81970202), and The National Key Research and Development Program of China–Traditional Chinese Medicine Modernization Research project 2017YFC1702000 (2017YFC1702003). Natural Science Foundation of Heilongjiang province (LC2018034).

AUTHOR CONTRIBUTIONS

Ying Zhang and YYZ conceived and designed all experiments. QQL, XWY, YYW, and HDL conducted diabetic wound healing model. MYZ, DHL, YYZ and ZWP identified the EPCs function in vivo and in vitro. YYZ, QQL, LJ, LHS conducted MicroPET/CT. YYZ, LNX, YCS, MML, MYG, XFZ, YMZ, ZGL, ZYT, YYZ, QY, and YQL performed all of the other experiments in this study. YYZ, Ying Zhang, LJ, XL, Yong Zhang and BFY discussed the data and wrote this paper.

ADDITIONAL INFORMATION

Supplementary information The online version contains supplementary material available at https://doi.org/10.1038/s41401-022-01013-2.

Competing interests: The authors declare no competing interests.

REFERENCES

1. Roop D. Defects in the barrier. Science. 1995;267:474–5.
2. Pober JS, Min W, Bradley JR. Mechanisms of endothelial dysfunction, injury, and death. Annu Rev Pathol. 2009;4:71–95.
3. Watt SM, Pleat JM. Stem cells, niches and scaffolds: applications to burns and wound care. Adv Drug Deliv Rev. 2018;123:82–106. 1
4. Wukich DK. Diabetes and its negative impact on outcomes in orthopaedic surgery. World J Orthop. 2015;6:331–9.
5. Wukich DK, Raspovic KM, Suder NC. Patients with diabetic foot disease fear major lower-extremity amputation more than death. Foot Ankle Spec. 2017: 1938640017694722.
6. Robbins JM, Strauss G, Aron D, Long J, Kuba J, et al. Mortality rates and diabetic foot ulcers: is it time to communicate mortality risk to patients with diabetic foot ulceration? J Am Podiatr Med Assoc. 2008;98:489–93.
7. Armstrong DG, Boulton AJM, Bus SA. Diabetic foot ulcers and their recurrence. N Engl J Med. 2017;376:2367–75.
8. Shen Y, Guo Y, Mikus P, Sulniute R, Wilczynska M, Ny T, et al. Plasminogen is a key proinflammatory regulator that accelerates the healing of acute and diabetic wounds. Blood. 2012;119:5879–87.
9. Martino MM, Tortelli F, Mochizuki M, Traub S, Ben-David D, Kuhn GA, et al. Engineering the growth factor microenvironment with fibronectin domains to promote wound and bone tissue healing. Sci Transl Med. 2011;3:100ra89.
10. Kronemann N, Bouloumi A, Bassus S, Kirchmaier CM, Busse R, Schini-Kerth VB. Aggregating human platelets stimulate expression of vascular endothelial growth factor in cultured vascular smooth muscle cells through a synergistic effect of transforming growth factor-beta 1 and platelet-derived growth factor (AB). Circulation. 1999;100:855–60.
11. Sunderkotter C, Goebeler M, Schulze-Osthoff K, Bhardwaj R, Sorg C. Macrophage-derived neovascularization factors. Pharmacol Ther. 1991;51:195–216.
12. De Palma M, Biziato D, Petrova TV. Microenvironmental regulation of tumour neovascularization. Nat Rev Cancer. 2017;17:457–74.
13. Bose D, Meric-Bernstam F, Hofstetter W, Reardon DA, Flaherty KT, Ellis LM. Vascular endothelial growth factor targeted therapy in the perioperative setting: implications for patient care. Lancet Oncol. 2010;11:373–82.
14. Kundra V, Escobedo JA, Kazlauskas A, Kim HK, Rhee SG, Williams LT, et al. Regulation of chemotaxis by the platelet-derived growth factor receptor-beta. Nature. 1994;367:474–6.
15. Robson MC, Phillips LG, Thomason A, Robson LE, Pierce GF. Platelet-derived growth factor BB for the treatment of chronic pressure ulcers. Lancet. 1992;339:23–25.
16. Katsimpardi L, Litterman NK, Schein PA, Miller CM, Loffredo FS, Wojtkiewicz GR, et al. Vascular and neurogenic rejuvenation of the aging mouse brain by young systemic factors. Science. 2014;344:630–4.
17. Loffredo FS, Steinhauser ML, Jay SM, Gannon J, Pancoast JR, Yalamanchi P, et al. Growth differentiation factor 11 is a circulating factor that reverses age-related cardiac hypertrophy. Cell. 2013;153:828–39.
18. Leinwand LA, Harrison BC. Young at heart. Cell. 2013;153:743–5.
19. Egerman MA, Cadena SM, Gilbert JA, Meyer A, Nelson HN, Swalley SE, et al. GDF11 increases with age and inhibits skeletal muscle regeneration. Cell Metab. 2015;22:164–74.
20. Smith SC, Zhang X, Zhang X, Gross P, Starosta T, Mohsin S, et al. GDF11 does not rescue aging-related pathological hypertrophy. Circ Res. 2015;117:926–32.
21. Poggioli T, Vujic A, Yang P, Macias-Trevino C, Uygur A, Loffredo FS, et al. Circulating growth differentiation factor 11/8 levels decline with age. Circ Res. 2016;118:29–37.
22. Du GQ, Shao ZB, Wu J, Yin WJ, Li SH, Wu J, et al. Targeted myocardial delivery of GDF11 gene rejuvenates the aged mouse heart and enhances myocardial regeneration after ischemia-reperfusion injury. Basic Res Cardiol. 2017;112:7.
23. Finkenzeller G, Stark GB, Strassburg S. Growth differentiation factor 11 supports migration and sprouting of endothelial progenitor cells. J Surg Res. 2015;198:50–6.
24. Boucher JM, Clark RP, Chong DC, Citrin KM, Wylie LA, Bautch VL. Dynamic alterations in decoy VEGF receptor-1 stability regulate neovascularization. Nat Commun. 2017;8:15699.
25. Eming SA, Martin P, Tomic-Canic M. Wound repair and regeneration: mechanisms, signaling, and translation. Sci Transl Med. 2014;6:265sr6.
26. Gawaz M, Vogel S. Platelets in tissue repair: control of apoptosis and interactions with regenerative cells. Blood. 2013;122:2550–4.
27. Li Q, Jiao L, Shao Y, Li M, Gong M, Zhang Y, et al. Topical GDF11 accelerates skin wound healing in both type 1 and 2 diabetic mouse models. Biochem Biophys Res Commun. 2020;529:7–14.
28. Guo W, Feng JM, Yao L, Sun L, Zhu GQ. Transplantation of endothelial progenitor cells in treating rats with IgA nephropathy. BMC Nephrol. 2014;15:110.
29. Yi DA, Thomas EU, Alexandra G, Amy J, Alla D. Angiogenic potential of cryopreserved amniotic membrane is enhanced through retention of all tissue components in their native state. Adv Wound Care. 2015;4:513–22.
30. Zhang YH, Cheng F, Du XT, Gao JL, Xiao XL, Li N, et al. GDF11/BMP11 activates both smad1/5/8 and smad2/3 signals but shows no significant effect on proliferation and migration of human umbilical vein endothelial cells. Oncotarget. 2016;7:12063–74.
31. Chung AS, Ferrara N. Developmental and pathological angiogenesis. Annu Rev Cell Dev Biol. 2011;27:563–84.
32. Belting M, Dorrell MI, Sandgren S, Aguilar E, Ahamed J, Dorfleutner A, et al. Regulation of neovascularization by tissue factor cytoplasmic domain signaling. Nat Med. 2004;10:502–9.
33. Patan S. Vasculogenesis and angiogenesis. Cancer Treat Res. 2004;117:3–32.
34. Rana D, Kumar A, Sharma S. Endothelial progenitor cells as molecular targets in vascular senescence and repair. Curr Stem Cell Res Ther. 2018;13:438–46.
35. Aday S, Zoldan J, Besnier M, Carreto L, Saif J, Fernandes R, et al. Synthetic microparticles conjugated with VEGF165 improve the survival of endothelial progenitor cells via microRNA-17 inhibition. Nat Commun. 2017;8:747.
36. Sawada N, Jiang A, Takizawa F, Safdar A, Manika A, Tesmenitsky Y, et al. Endothelial PGC-1alpha mediates vascular dysfunction in diabetes. Cell Metab. 2014;19:246–58.
37. Lerman OZ, Greives MR, Singh SP, Thanik VD, Chang CC, Seiser N, et al. Low-dose radiation augments vasculogenesis signaling through HIF-1-dependent and -independent SDF-1 induction. Blood. 2010;116:3669–76.
38. Kaur S, Tripathi D, Dongre K, Garg V, Rooge S, Mukopadhyay A, et al. Increased number and function of endothelial progenitor cells stimulate neovascularization by resident liver sinusoidal endothelial cells (SECs) in cirrhosis through paracrine factors. J Hepatol. 2012;57:1193–8.
39. Krishnamurthy P, Thal M, Verma S, Hoxha E, Lambers E, Ramirez V, et al. Interleukin-10 deficiency impairs bone marrow-derived endothelial progenitor cell survival and function in ischemic myocardium. Circ Res. 2011;109:1280–9.

40. Fadini GP, Boscaro E, Albiero M, Menegazzo L, Frison V, de Kreutzenberg S, et al. The oral dipeptidyl peptidase-4 inhibitor sitagliptin increases circulating endothelial progenitor cells in patients with type 2 diabetes: possible role of stromal-derived factor-1alpha. Diabetes Care. 2010;33:1607–9.
41. Harmon EB, Apelqvist AA, Smart NG, Gu X, Osborne DH, Kim SK. GDF11 modulates NGN3^{+} islet progenitor cell number and promotes beta-cell differentiation in pancreas development. Development. 2004;131:6163–74.
42. Li H, Li Y, Xiang L, Zhang J, Zhu B, Xiang L, et al. GDF11 attenuates development of type 2 diabetes via improvement of islet beta-cell function and survival. Diabetes. 2017;66:1914–27.
43. Rezende F, Moll F, Walter M, Helfinger V, Hahner F, Janetzko P, et al. The NADPH organizers NoxO1 and p47phox are both mediators of diabetes-induced vascular dysfunction in mice. Redox Biol. 2017;15:12–21.
44. Safar ME. Arterial stiffness as a risk factor for clinical hypertension. Nat Rev Cardiol. 2018;15:97–105.
45. Tanaka R, Vaynrub M, Masuda H, Ito R, Kobori M, Miyasaka M, et al. Quality-control culture system restores diabetic endothelial progenitor cell vasculogenesis and accelerates wound closure. Diabetes. 2013;62:3207–17.
46. Gallagher KA, Liu ZJ, Xiao M, Chen H, Goldstein LJ, Buerk DG, et al. Diabetic impairments in NO-mediated endothelial progenitor cell mobilization and homing are reversed by hyperoxia and SDF-1 alpha. J Clin Invest. 2007;117:1249–59.
47. Takeda N, Maemura K, Imai Y, Harada T, Kawanami D, Nojiri T, et al. Endothelial PAS domain protein 1 gene promotes neovascularization through the transactivation of both vascular endothelial growth factor and its receptor, Flt-1. Circ Res. 2004;95:146–53.
48. Chen L, Endler A, Uchida K, Horiguchi S, Morizane Y, Iijima O, et al. Int6/eIF3e silencing promotes functional blood vessel outgrowth and enhances wound healing by upregulating hypoxia-induced factor 2 alpha expression. Circulation. 2010;122:910–9.
49. Ozawa K, Kondo T, Hori O, Kitao Y, Stern DM, Eisenmenger W, et al. Expression of the oxygen-regulated protein ORP150 accelerates wound healing by modulating intracellular VEGF transport. J Clin Invest. 2001;108:41–50.
50. Yang Y, Huang K, Wang M, Wang Q, Chang H, Liang Y, et al. Ubiquitination flow repressors: enhancing wound healing of infectious diabetic ulcers through stabilization of polyubiquitinated hypoxia-inducible factor-1α by theranostic nitric oxide nanogenerators. Adv Mater. 2021;33:e2103593.
51. Ii M, Takeshita K, Ibusuki K, Luedemann C, Wecker A, Eaton E, et al. Notch signaling regulates endothelial progenitor cell activity during recovery from arterial injury in hypercholesterolemic mice. Circulation. 2010;121:1104–12.
52. Dai X, Yan X, Zeng J, Chen J, Wang Y, Chen J, et al. Elevating CXCR7 improves angiogenic function of EPCs via Akt/GSK-3beta/Fyn-mediated Nrf2 activation in diabetic limb ischemia. Circ Res. 2017;120:e7–e23.
53. Li FY, Lam KS, Tse HF, Chen C, Wang Y, Vanhoutte PM, et al. Endothelium-selective activation of AMP-activated protein kinase prevents diabetes mellitus-induced impairment in vascular function and reendothelialization via induction of heme oxygenase-1 in mice. Circulation. 2012;126:1267–77.
54. Hiesinger W, Perez-Aguilar JM, Atluri P, Marotta NA, Frederick JR, Fitzpatrick JR, et al. Computational protein design to reengineer stromal cell-derived factor-1alpha generates an effective and translatable angiogenic polypeptide analog. Circulation. 2011;124:S18–26.
55. Climent M, Quintavalle M, Miragoli M, Chen J, Condorelli G, Elia L. TGFβ triggers mir-143/145 transfer from smooth muscle cells to endothelial cells, thereby modulating vessel stabilization. Circ Res. 2015;116:1753–64.
56. Wang W, Qu R, Wang X, Zhang M, Zhang Y, Chen C, et al. GDF11 antagonizes psoriasis-like skin inflammation via suppression of NF-κB signaling pathway. Inflammation. 2019;42:319–30.
57. Kanitkar M, Jaiswal A, Deshpande R, Bellare J, Kale VP. Enhanced growth of endothelial precursor cells on PCG-matrix facilitates accelerated, fibrosis-free, wound healing: a diabetic mouse model. PLoS One. 2013;8:e69960.
58. Nishimura Y, Ii M, Qin G, Hamada H, Asai J, Takenaka H, et al. CXCR4 antagonist AMD3100 accelerates impaired wound healing in diabetic mice. J Invest Dermatol. 2012;132:711–20.